9-1-2010

Drive and Motion Design In Material Handling Equipment

Jorg Oser
TU Graz Austria

Christian Landschutzer
TU Graz Austria

DRIVE AND MOTION DESIGN IN MATERIAL HANDLING EQUIPMENT

Jörg Oser, Christian Landschützer
TU Graz, Austria

Abstract

Drives account in many cases up to one third of the costs of material handling equipment. This fact justifies a closer look to important drive and motion issues. Typical design criteria for drives are energy and power consumption, wear, heat and noise generation. Engineering design activities start with the generation of the system configuration, that is to make appropriate topological decisions where to locate the drives in the equipment structure. These decisions define to a great extent the functional quality of the mechanical structure and the distribution of forces in the power train. For early design stages an elasto-kinetic model is developed, which is later enhanced by a more detailed simulation model. Another important issue is the definition of high quality motion profiles defined by selected velocity-time relationships.

1 Introduction

In many cases an excentric location of the drives is necessary due to maintenance and repair accessibility and also for ease of equipment assembly. Here a wider class of excentric drive arrangements is investigated with a general mechanical model. This model is valid for vertical arrangements encountered in carousels as well as for horizontal conveyors with two tension members. The model contains the equation of motions and deformations and their influence on the distribution of the driving forces in the power train.

Another question is the achievement of high quality motion performance. The criteria of high quality motion systems are the accuracy of the motion profile, precision of the sequence of motions, assurance of low vibration induction, high energy efficiency and limitation of admissible stress in the electromechanical system called power train.

In the paper we investigate three different motion profiles with a generally applicable method to evaluate their performance related to peak torque, energy efficiency, jerk free and jerk limited motion parameters. Parameters are used to describe tradeoffs between

peak torque positioning and jerk free motion for soft moves as well as low energy consumption.

This paper contains six sections. In the first section we present an introduction and problem statement. The second section contains the investigation of the drive location problems. Here our theoretical model of an excentric drive configuration and the associated equations of motion are presented. The third section contains the influence of quality motion profiles in the drive selection process. The fourth and the fifth section present a more detailed multibody simulation model and the results for selected motion profiles and a discussion of the tradeoffs according to design criteria. The final section contains a summary plus literature references.

2 Drive Location

The first question deals with the location of a drive in conveying units. Fig. 1 shows a common application of the drive unit in an excentric position on the drive shaft as presented in [1].

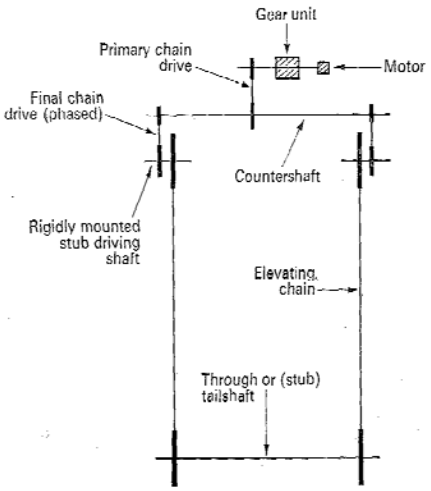

Figure 1: Conveyor Drive Arrangement.

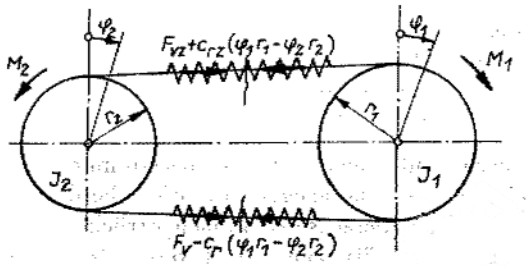

Figure 2: Belt Drive Model.

Regarding a side view of Fig.1 in the arrow direction of the elevating chain leads to Fig. 2 of the dynamic conveyor model presented as belt drive model in [2].

An excentric location has several advantages such as easy access for assembly and maintenance, reduction of product contamination due to wear and more rigidity and better stability with respect to dynamic motions of the system. In fact the system as shown in Fig. 1 is quite general in its possible range of applications.

Fig. 1 could be a chain conveyor with horizontal drive shafts. Fig. 1 could also be a carousel structure with vertical shafts. In both cases it is important to know the distribution of forces in the shafts and the tension members like chains or tooth belts

resulting from elastic deformations of the exposed members during power transmission. In most cases designers are unaware or neglect the substantial influence of the excentric drive location, which is investigated in this paper.

Thus the mechanical structure consists of the drive unit, two shafts and two tension members either in a horizontal or vertical arrangement depending on the material handling equipment.

The main dynamic motions of mass 1 are the angle φ_1 and of mass 2 angle φ_2. The equations of motions are

$$I_1\ddot{\varphi}_1 + \left(c_{rz} + c_r\right) r_1 \left(\varphi_1 r_1 - \varphi_2 r_2\right) = M_1 - r_1\left(F_{vz} - F_v\right) \tag{1}$$

$$I_2\ddot{\varphi}_2 + \left(c_{rz} + c_r\right) r_2 \left(\varphi_2 r_2 - \varphi_1 r_1\right) = -M_2 + r_2\left(F_{vz} - F_v\right) \quad \text{with} \tag{2}$$

$I_{1,2}$ [kgm^2]	rotational moments of inertia
$M_{1,2}$ [Nm]	torques at shafts 1,2
$\ddot{\varphi}_{1,2}$ [1/s^2]	angular accelerations
c_{rz}, c_r [N/m]	rigidity of tension members
F_{vz}, F_v [N]	pretension forces
$r_{1,2}$ [m]	pulley radius

Considering only stationary forces and symmetry in stiffness and geometry in the preliminary design stage leads to the assumptions $I_{1,2} = 0$, $F_{vz} = F_v$, $c_{rz} = c_r$ equal longitudinal stiffnesses of tight and slack side, $r_1 = r_2 = R$ equal pulley radius resulting from (1) and (2).

$$4c_r R^2\left(\varphi_1 - \varphi_2\right) = M_1 + M_2 = F_1 R + F_2 R \tag{3}$$

$$\Delta\varphi_{12} = \frac{\left(F_1 + F_2\right) L}{4REA} \tag{4}$$

Thus the relative angular displacement is $\Delta\varphi_{12} = \varphi_1 - \varphi_2$ with $c_r = c_s/L = EA/L$ where c_s is the specific tensional rigidity of the chain, tooth belt or alike.

Fig. 1 exhibits the following data

EA [N]	longitudinal stiffness of tension member (belt, chain)
L [m]	distance between drive and reverse shaft
H_u [m]	shorter (left) distance between primary chain drive and sprocket
H_o [m]	longer (right) distance between drive and sprocket
$H_2 = H_o + H_u$ [m]	horizontal distance between chains (tension members)
$J_{o,u,2}$ [m^4]	geometrical moment of inertia with indices from above
$F_{1,2}$ [N]	circumferential forces corresponding to torques $M_{1,2}$
F_w [N]	external forces each acting on one chain (tension) member resulting from friction and inertial forces
G [N/m^2]	shear modulus of shafts

Thus the total driving force acting on the left and right driving pulley equals

$$F_{1u} + F_{1o} = 4F_w \tag{5}$$

Furthermore from Fig. 2 both pulleys are subject to circumferential forces $F_{1,2}$ corresponding to torques $M_{1,2}$

$$F_{1u} = F_{2u} + 2F_w \quad \text{wherefrom} \quad F_{2u} = F_{1u} - 2F_w \quad \text{and} \quad F_{2u} = F_{2o} \tag{6}$$

The basic law of torsional deformation of shafts follows from elasticity theory with

$$\Delta\varphi_1 = M_1 H / GJ \tag{7}$$

Applying this law to all members of the power train contributing to torsional deformation for the left belt (chain) model u and setting this equal to the total deformation of the right pulley model o results in

$$\Delta\varphi_{1u} + \Delta\varphi_{12u} + \Delta\varphi_{2u} = \Delta\varphi_{1o} + \Delta\varphi_{12o} \tag{8}$$

Here $\Delta\varphi_{12}$ is the angle of torsional deformation between pulleys 1,2 due to the longitudinal elastic deformation of the tension members from (4).

$$\Delta\varphi_{12u} = \frac{(F_{1u} + F_{2u})L}{4REA} \quad \text{and} \quad \Delta\varphi_{12o} = \frac{(F_{1o} - F_{2o})L}{4REA} \tag{9}$$

This angle needs to be added to the torsional deformation of the shafts. Inserting equation (7) and (9) into (8) leads to

$$\frac{F_{1u}RH_u}{GJ_u} + \frac{(F_{1u} + F_{2u})L}{4REA} + \frac{F_{2u}RH_2}{GJ_2} = \frac{F_{1o}RH_o}{GJ_o} + \frac{(F_{1o} - F_{2o})L}{4REA} \tag{10}$$

Substituting (6) into (10), reducing R/G and replacing F_{1o} from (5) results in

$$F_{1u} = 2F_w \frac{2 + \frac{LGJ_o}{R^2EAH_o} + \frac{H_2}{J_2}\frac{J_o}{H_o}}{1 + \frac{LGJ_o}{R^2EAH_o} + \frac{H_u}{J_u}\frac{J_o}{H_o} + \frac{H_2}{J_2}\frac{J_o}{H_o}} = 2F_w \frac{2 + 2K + H}{2K + 2H} \quad \text{with } H = H_2/H_o \tag{11}$$

Substituting (11) into (5) leads to the relation of the circumferential forces

$$\frac{F_{1u}}{F_{1o}} = \frac{1 + \frac{LGJ_o}{2R^2EAH_o} + \frac{H_2}{2J_2}\frac{J_o}{H_o}}{\frac{LGJ_o}{2R^2EAH_o} + \frac{H_2}{2J_2}\frac{J_o}{H_o} + \frac{H_u}{J_u}\frac{J_o}{H_o}} = \frac{1 + K + H/2}{K + H/2 + H - 1} = \frac{2 + 2K + H}{2K + 3H - 2} \tag{12}$$

If the drive is located completely left, $H_u = 0$ and $H_2 = H_o$ with $J_o = J_u = J_2$

$$\frac{F_{1u}}{F_{1o}} = \frac{K + 1.5}{K + 0.5} \quad \text{with} \quad K = \frac{LGJ_o}{2R^2EAH_o} \tag{13}$$

results in a hyperbolic function. With K = 1.5 – 4.5 in industrial applications F_{1u}/F_{1o} varies between 1.5 and 1.2.

If the drive is located in the middle between the two tension members, $H_o = H_u = H_2/2$ then

$$\frac{F_{1u}}{F_{1o}} = \frac{1+K+1}{K+1+1} = 1$$

with equal circumferential forces.

The conclusion is that drive forces can be 20 % to 50 % higher on this side, where the drive is located closer to the tension member. Thus an excentric drive arrangement needs a careful calculation of the forces acting on the two tension members differently.

3 Laws of Motion

Moving a mass *M* along a distance *s* within a time *T* can be performed with different laws of motion. Modern type inverters allow virtually any possible motion type. The most well known is a linear velocity time relationship shown in Fig. 3 with linear acceleration, a constant speed interval and linear deceleration similar to an extension.

Three issues are treated here:

- Which function should be chosen for acceleration/deceleration?
- How can the travel time *T* be calculated?
- How long should the acceleration phase be if power installation is to be minimized?

linear	quadratic	sinus-square
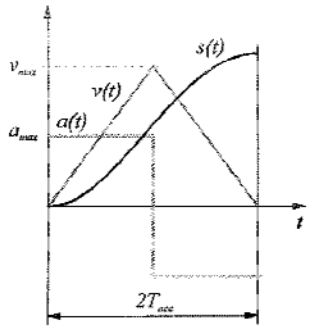	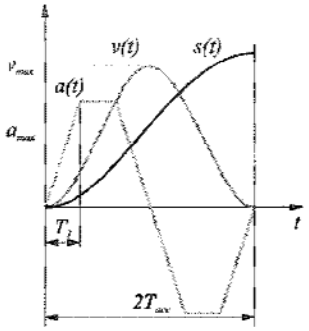	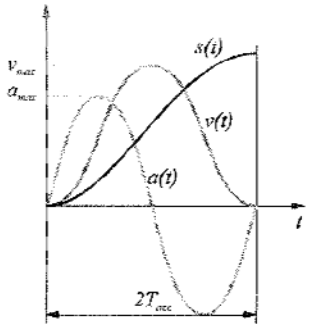
velocity: $v_{(t)} = at$	$v_{(t)} = at^2/2T_1$	$v_{(t)} = a/\omega \sin^2(\omega t)$
acceleration: $a/\bar{a} = 1$	$a/\bar{a} = \frac{1}{1 - T_1/T_{acc}}$	$a/\bar{a} = \pi/2$
jerk: $da/dt = \infty$	$da/dt = a/T_1$	$da/dt = a\,\pi/T_{acc}$

Figure 3: Various Speed Profile.

If constant speed is neglected three speed diagrams describe possible acceleration/ deceleration functions. The table shows that the maximum acceleration a related to the average $\bar{a}$ depends on the type of the speed function and varies between 1 and 1.57 and is minimal for the linear profile. However this advantage is counteracted by an infinite jerk da/dt, which gives rise to substantial vibrations in the power train. Using quadratic or sinus-squared speed profiles, limits these vibrations due to a softer rise of acceleration. For a final answer a simulation model can be evaluated as shown in the next section.

Calculating travel times T for the different speed profiles and a predetermined distance s is simplified extremely when using symmetrical acceleration f_1/deceleration f_3 as shown in Fig. 4.

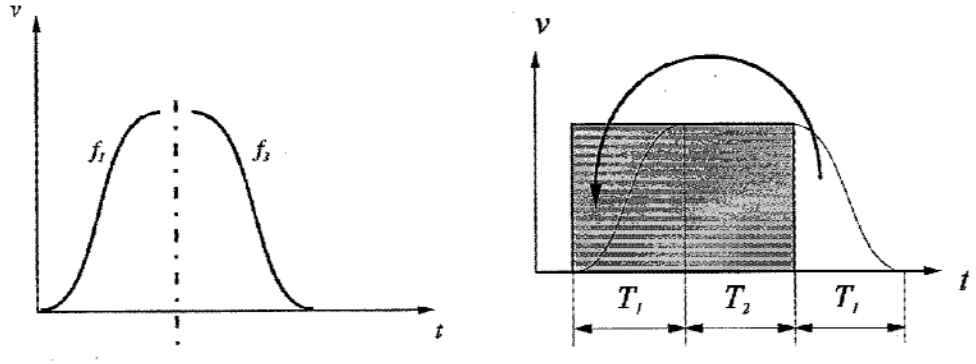

Figure 4: Symmetric Speed Profiles.

$$T = 2\sqrt{sT_{acc}/v_{\max}} \quad \text{if} \quad s \le v_{\max}T_{acc} \qquad T_1 = T_{acc}$$

$$T = s/v_{\max} + T_{acc} \quad \text{if} \quad s \ge v_{\max}T_{acc} \tag{14}$$

A solution how long the acceleration time should be has been proposed in [4] for constant acceleration and is generalized here for the linear speed profile. x is the percentage of the total travel time T to be determined for minimum power consumption. Then acceleration $a = v_{max}/(xT)$, inertial forces $F_{max} = aM = Mv_{max}/(xT)$, maximum speed $v_{max} = s/T(1 - x)$, which is independent of the speed profile.

Deriving the power necessary for traveling a distance s in time T with a mass M

$$P_{\max} = F_{\max}v_{\max} \tag{15}$$

$$P_{\max} = Mv_{\max}^2/(xT) = \frac{Ms^2}{T^3}\frac{1}{x(1-x)^2} \tag{16}$$

Searching the minimum of P_{max} with

$$\frac{dP_{\max}}{dx} = 0 \quad \text{leads to} \quad x = 1/3.$$

That means when choosing acceleration time on third of total travel time the minimum power installation is achieved.

4 Multibody Simulation Model

4.1 Basic Relations

In section 2 an elasto-kinetic model revealed the distribution of forces due to an excentric drive location. Its limitations are, however, that dynamic forces can be considered only very generally. Therefore this second part of the paper presents a reference design process for dynamical systems design in an early design stage, focusing on machinery part design for low cycle fatigue and thermal design of electrical drives on a rotating shelf storage system (carousel storage). Similar models can be developed for other equipment types and be adapted to various scenarios, describing customer wishes. The overall goal should be a library of simulation models, which can be easily extended and adapted to varying conditions.

Basic criteria to describe drive efficiencies are effective torque, power consumption and cubic torque calculation for mechanical durability of parts. A classic method to calculate time-dependent loading for thermal and mechanical processes is now shown. The so called effective moment M_{eff} describes thermal loading by adding time-dependent motor torque quadratically.

$$M_{eff} = \sqrt{\frac{1}{2T_{acc}} \int_0^{2T_{acc}} M(t)^2 \, dt} \qquad for \;\; 0 \le t \le 2T_{acc} \tag{17}$$

$$n_{eff} = \frac{1}{2T_{acc}} \int_0^{2T_{acc}} n(t) \, dt \qquad for \;\; 0 \le t \le 2T_{acc} \tag{18}$$

Multiplied by an average speed of rotation n_{eff} the effective power P_{eff} can be calculated. It represents the nominal load or power an electric drive can deliver. Considering the duration of loading leads to operation classes (S1, S3,…). Thus the average power P_{eff} must be smaller than nominal power P_{nom}.

$$P_{eff} = M_{eff,shaft}(2T_{acc})\, 2\pi n_{eff} \tag{19}$$

$$P_{eff} \le P_{nom.} \tag{20}$$

Mechanical durability is calculated from a simplified approach of Miner's damage accumulation theory. This approach uses a cubic equivalent torque M_{cub} for reducing variable actual loads to one single value. The actual load as a single value from a cubic mean is compared to nominal value (by a cubic relation) known from component suppliers for durable operation.

$$M_{cub} \geq \sqrt[3]{\frac{1}{2T_{acc}} \int_0^{2T_{acc}} \left| M(t)^3 \right| dt} \quad for \quad 0 \leq t \leq 2T_{acc} \tag{21}$$

So for easy early stage accurate dimensioning the following two equations must be fulfilled, where *M(t)* comes from simulation and M_{nom} and M_{max} are given by manufacturers of certain parts or from experimental investigations.

$$M_{cub} \leq M_{nom} \tag{22}$$

$$MAX\left(M(t)\right) \leq M_{max} \tag{23}$$

The following two basic equations specify power and energy in the system and are basic for some later results.

$$P = M_{shaft}\, \omega_{shaft} \tag{24}$$

$$E = \int_0^{2T_{acc}} P\, dt \tag{25}$$

4.2 Description of Components

The major parts of the system are according to Fig. 5 and Fig. 7:

- Distance controlled drive torque using various drive strategies (equations 28-29).
- Elastic shafts. Elasticity and damping from geometry and material.
- Masses and inertias. Parameters from CAD.
- Pulleys. Radius from manufacturer.
- Friction moments and forces, representing real energy dissipation. Assumption based on general efficiency.
- Upper and lower tooth belts divided into small parts length *l*, with Young's module *E* and cross section *A*, which can only build up tension forces and do not have stiffness (or very small stiffness modeled for numerical reasons) against pressure forces. This detection is controlled by measurement of elongation. c_{Belt} corresponds to c_r in (3)

$$c_{Belt} = \begin{cases} \dfrac{EA}{l} & for\ pos.elongation \\ \dfrac{EA}{10000\, l} & for\ zero\ and\ neg.el. \end{cases} \tag{26}$$

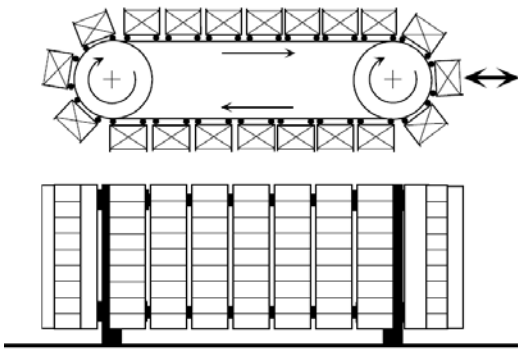

Figure 5: Carousel.

- Tooth belt pretension. Modeled by an initial distance and initializing simulation afterwards.
- Twist force, representing the carrier which is connected to the lower and the upper belt and therefore can not twist ore rotate. As small rotation is possible due two manufacturing tolerances, twist force $F_{twist,i}$ of carrier i follows a nonlinear law using the difference of absolute position of upper and lower mass $x_{up,i}$ and $x_{down,i}$ which are representing the whole carrier i. factors f, f_2 and exponent tw follow estimations and the absolute real possible difference of $x_{up,i}$ and $x_{down,i}$.

$$F_{twist,i} = f\,\Delta x_i + \left(f_2\,\Delta x_i\right)^{tw} \qquad with: \quad \Delta x_i = x_{up,i} - x_{down,i} \tag{27}$$

- Some functions to calculate equations (20-21).

4.3 Simulation Approach

There are many ways to build up mechanical dynamical models with modern CAE and MBS techniques. Two different approaches are described here. One is a mechanical system formulation by the classic Newton or Lagrange approach which delivers sets of differential equations. Solving them is only in few cases possible by analytic methods, so there is a set of software to do this numerically. As well known tool is MATLAB/Simulink software which offers possibilities in nearly all fields of technical calculation in a very general way. A standard way of description is the signal-flow-based way, using a block diagram (Fig. 6, left).

On the other hand there is a library based object oriented way using a graphical modeling language in form of drag & drop. A very powerful product is ITI-Sim [6] and in its later extended releases Simulation X (Fig. 6, right). The major difference is not in solving the equations but in building the models, in a more engineering like process.

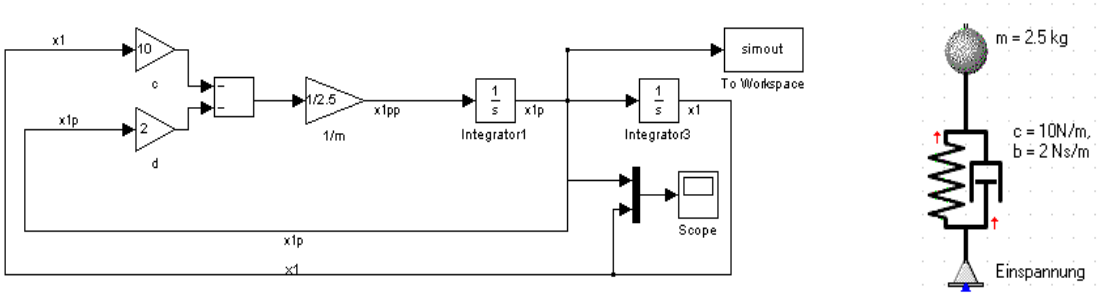

Figure 6: One-Mass-Oscillator modeled in MATLAB/Simulink and ITI-Sim.

The carousel storage system now is modeled and described as follows. Two revolving tooth belts pull the load carriers which are driven by elastic shafts and rigid pulleys. The

two belts are coupled by the drive shaft, which is divided into an upper and lower part, and the reverse shaft. The tooth belt is represented by linear springs with viscous damping, divided into small parts between one and the following carriers. Fig. 7 exhibits the simulation model of the carousel storage system.

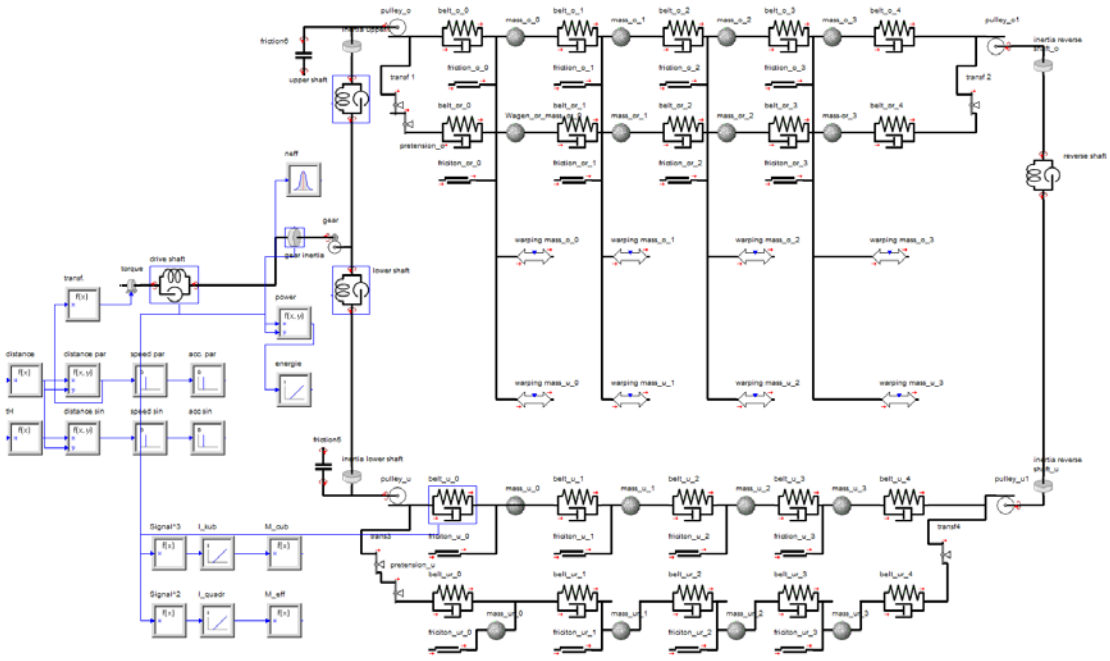

Figure 7: Carousel Storage System Modeled in ITI-Sim.

5 Drive Train Simulation

The following calculations were made when calculating mechanical properties in solving the simulation model with some simplifying assumptions.

5.1 Dynamic Force Calculation of Carousel System

The following section describes the dynamic situation in the system resulting in effective and cubic moments of drives and mechanical part operated with a linear velocity profile.

Taking a closer look to the dynamic loading of lower and upper shaft (Fig. 8) which drives the tooth belt pulley there is a factor of 2651/1520 = 1.74 representing the maximum torque during acceleration higher than the average torque for acceleration of the rigid system as calculated before. Neglecting the influence of the dynamic system, modeled by several elastic subsystems, can lead to inappropriate weak parts that would not endure the proposed lifetime. So if equation 23 is fulfilled and the cubic moment (1579 Nm) is appropriate to the nominal moment (22) one can be sure to have well designed parts for early stage dimensioning the whole machine.

Taking into account only quasistatic manual calculation (12) delivers a factor 2.38 for the relation between F_{1u}/F_{1o} where simulation model shows 3.70. The difference results from the simplier modeling for the analytical way, which does not consider influences like twist force (27), models only a rigid system and has no influence of discrete mass distribution over the tooth belt length.

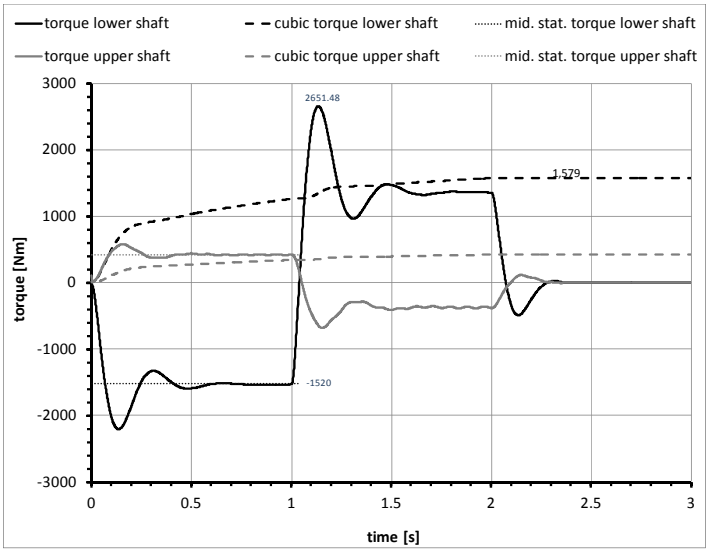

Figure 8: Dynamic Torques at Upper and Lower Shaft.

5.2 Influence of Motion Velocity Profile

Equations for two common known drive strategies to get masses into motion are presented in [5] investigating a one-mass oscillation system. The parabolic distance profile (linear velocity) results into rectangular accelerations causing impacts to the mass. Analogue to figure 3 the distance calculates with $H = s(2T_{acc})$:

$$s_{lin} = \begin{cases} 2H\left(\dfrac{t}{2T_{acc}}\right)^2 & for\ \ 0 \le t \le T_{acc} \\ H - 2H\left(\dfrac{t-2T_{acc}}{2T_{acc}}\right)^2 & for\ \ T_{acc} \le t \le 2T_{acc} \end{cases} \tag{28}$$

An optimization step is to use distance functions with higher derivations by the use of a sinusoidal profile (sin). Ref. [3] shows a collection of motion profiles.

$$s_{sin} = H\frac{t}{2T_{acc}} - \frac{H}{2\pi}\sin\left(\frac{2\pi t}{2T_{acc}}\right) \qquad for\ \ 0 \le t \le 2T_{acc} \tag{29}$$

Very valuable insights are offered by the dynamic model to investigate energy consumption where Fig. 9 shows interesting differences between “lin” and “sin” drive profile.

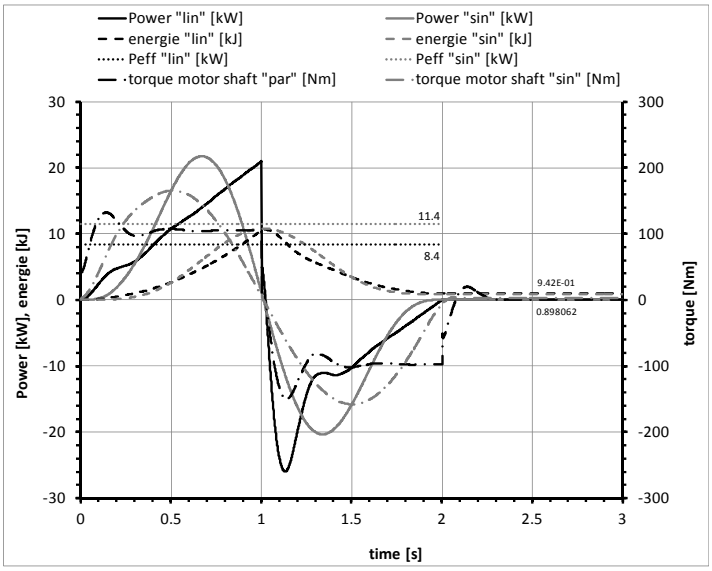

Figure 9: Comparison of Energies and Power for “lin” and “sin” Drive Profile.

Table 1: Comparison of Drive Profiles According to Fig. 9

	linear profile	sinusoidal profile
maximum motor power	-	smaller
effective motor power	smaller	-
maximum torque	smaller	-
energy consumption	smaller	-
energy loss (friction)	-	smaller

The direct comparison between the two presented drive profiles (Table 1) on a first look shows the linear profile to be better in two aspects. Also the fourth row in Table 1, describing the energy consumption after 2 s, is only smaller with “lin”-profile. The loss due to friction is nearly 4.5 % higher (0.94/0.9) for the linear profile. Finally “sin”-profile needs a larger drive (with more effective power and maximum torque) but is overall the better choice, because of jerk limitation.

Showing these considerations should inspire to investigate more common use profiles in further work, to find optimal drive strategies, based on simulative real dynamic conditions.

For dimensioning the thermal process in the electric drive Fig. 10 shows the relevant effective moment being 103 Nm to fulfill equations 20 (using 17-19). For the acceleration

the maximum power should not exceed P_{max} = 149 ·172 = 25.6 kW. Motor shafts dynamical loading has a dynamic load factor of about 149/105 = 1.42.

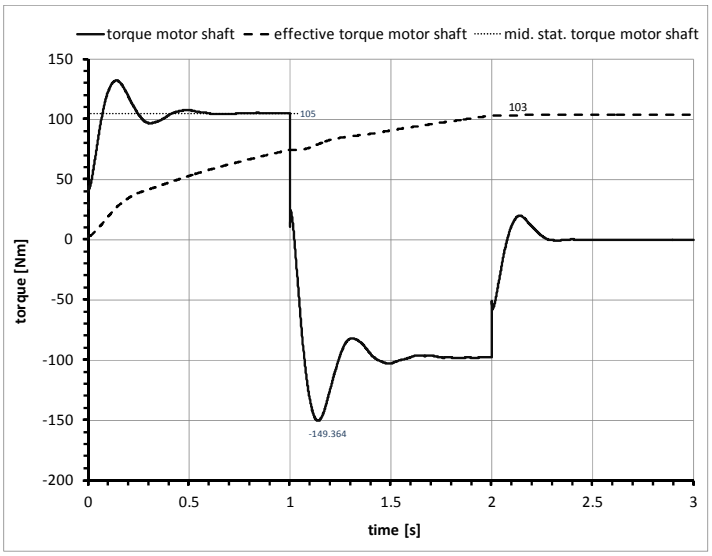

Figure 10: Dynamic Torques at Electrical Drive.

6 Summary

An analytical solution was presented to solve the drive location problem. A refined simulation model was developed to extend the static model with dynamic effects in order to avoid expensive iteration steps at later design stages. Furthermore this elementary model can help to understand and improve the whole system taking dynamic effects into account.

References

[1] Jones, L. (Ed.), *Mechanical Handling with Precision Conveyor Chain*, Hutchinson, London (1971).

[2] Holzweissig, F. and Dresig, H., *Lehrbuch der Maschinendynamik: Grundlagen und praxisorientierte Beispiele*, Fachbuchverlag, Leipzig (1994).

[3] Vössner, S., *Spielzeitberechnung von Regalförderzeugen*, Dissertation, Technische Universität, Graz (1994).

[4] Riese, S. and Kiel, E., "Der einfache und schnelle Weg zur perfekten Positionierung," *SPS/IPC/DRIVES 2008 Elektrische Automatisierung*, 279-287 (2008).

[5] Effenberger, W., "Konstruktionselement Bewegungsgesetz," *Antriebstechnik*, 38, 2, 59-63 (1999).

[6] ITI System Simulation, http://www.iti.de/ *(20.4.2010).*